A Survey on Iris Segmentation using Distantly Acquired Face Images

Senbhaga S

PG Scholar, Department of Computer Science-Software Engineering,

SNS College of Technology, Coimbatore-35

Email: senbhagait@gmail.com

ABSTRACT

Remote human identification using iris biometrics has high civilian and surveillance applications and its success requires the development of robust segmentation algorithm to automatically extract the iris region. This paper presents a new iris segmentation framework which can robustly segment the iris images acquired using near infrared or visible illumination. The proposed approach exploits multiple higher order local pixel dependencies to robustly classify the eye region pixels into iris or non iris regions. Face and eye detection modules have been incorporated in the unified framework to automatically provide the localized eye region from facial image for iris segmentation. We develop robust post processing operations algorithm to effectively mitigate the noisy pixels caused by the misclassification. Experimental results presented in this paper suggest significant improvement in the average segmentation errors over the previously proposed approaches, i.e., 47.5%, 34.1%, and 32.6% on UBIRIS.v2, FRGC, and CASIA.v4 at-a-distance databases, respectively. The usefulness of the proposed approach is also ascertained from recognition experiments on three different publicly available databases.

Keywords- **Biometrics, iris recognition, iris segmentation unconstrained iris recognition.**

IJSER

1. INTRODUCTION

IRIS RECOGNITION has been emerging as one of the most preferred biometric modalities for automated personal identification. Conventional near infrared (NIR)-based iris recognition systems are designed to work in strictly constrained environments in order to mitigate the influence of the noises from various sources such as illumination changes, occlusions from eyeglasses, eyelashes, hair, and reflections, just to name a few. The operating wavelength of the NIR used in such conventional systems is usually between 700 and 900 nm, which has been used to reveal iris texture and provide sufficient contrast 1 even for the darkly pigmented irises. NIR illumination must be used with precaution and complied with the safety regulations. Excessive level of the NIR illumination can cause permanent damage to human eyes as the nature of our human eyes is not instinctively responsive to the NIR illumination. Therefore, the iris images are usually acquired within a short distance between 1 and 3 ft as longer distances require stronger NIR illumination, which may harm our eyes. There have been some promising efforts to acquire iris images using visible illumination to overcome the limitations of current iris recognition systems using NIR-based acquisition and develop less cooperative iris recognition systems for higher security and surveillance applications. The use of visible wavelength (VW) imaging can address the shortcomings of acquisition using NIR-based imaging, especially when distant acquisition for iris images is required. The advanced imaging technologies, for example, high-resolution CMOS/CCD cameras, are now available to conveniently acquire high-resolution images at distances beyond 3 m using visible illumination and locate iris images suitable for recognition. Conventional iris recognition systems operate in stop-and-stare mode which requires significant cooperation from the users. The usage of visible imaging can relax such requirement and enable iris recognition in less cooperative environment using images acquired at further distance. Such iris recognition system can be a good candidate for high-security surveillance such as identifying suspected criminals from the crowd. In References there are two typical examples of the iris databases acquired using visible imaging, which are now available in the public domain to promote further research efforts in this area.

Iris images acquired using unconstrained visible imaging is significantly noisier than those acquired by the conventional iris recognition systems in the controlled environment. There can be multiple sources of commonly observed noise in such images, and common ones may result from blurring artefact caused by motion/defocus, occlusions from eyelashes, hair and eyeglasses, specular reflections, off-angles,

and partia images. Table I shows the comparative summary of the iris recognition at-a-distance using VW and NIR imaging.3 Fig. 1presents some noisy iris images which were acquired using visible imaging in unconstrained environments.

Integro-differential operator is perhaps the most widely used iris segmentation approach deployed in most of the commercial iris recognition systems. The operator and its variants have shown effectiveness to segmenting the iris images for NIR-acquired iris images in controlled environments. The operator works effectively when there is a significant contrast at the boundary of interest. There is typically more contrast at the pupillary boundary in NIR images than in visible light images.

TABLE I
COMPARATIVE SUMMARY OF IRIS RECOGNITION AT-A-DISTANCE WITH DIFFERENT IMAGING CONDITIONS

	VW	NIR wavelength
Remote surveillance	High	Low
Performance	Low	High
Applications	Forensics, surveillance	Commercial, high security
Imaging cost	Low	High
Image quality	Degraded due to noise	Good
Medical/health concern	Low	High
User cooperation	Low	High
Key challenges	**Robust iris segmentation, iris feature extraction**	Segmentation and recognition are quite matured

Fig. 1. Sample iris images acquired in unconstrained environments.

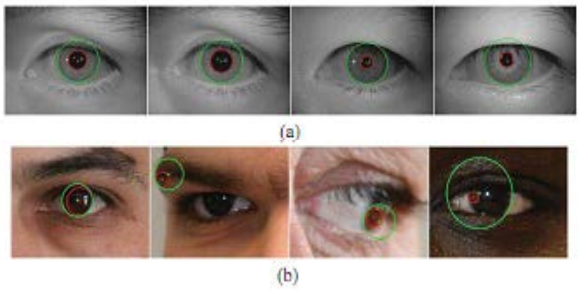

Fig. 2. Samples segmentation results from conventional iris segmentation approach applied on (a) NIR-acquired and (b) VW-acquired iris images.

Another promising approach was reported by using neural network (NN) to classify the image pixels. The presented approach consists of two sequential stages: 1) sclera and 2) iris training/classification stages. Both stages exploit the local colour features from hue, saturation, value and YCbCr colour spaces of the image.

2. IDENTIFICATION OF HUMAN AT A DISTANCE USING IRIS BIOMETRICS

Remote identification of human at-a-distance using iris biometrics requires development of completely automated algorithm, which can robustly segment the iris region from the distantly acquired facial images. Despite some initial efforts in segmenting the VW iris images acquired in unconstrained conditions, the segmentation accuracies of those methods are quite limited. This paper focuses on the aforementioned segmentation problem and develops a completely automated and unified approach to segmenting the iris region from the facial image at a distance acquired using VW and NIR imaging. The proposed approach works at pixel level by exploiting the localized Zernike moments

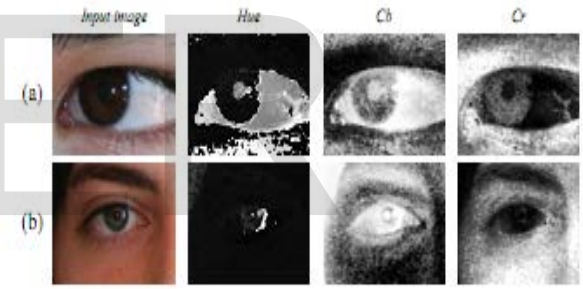

Fig. 3. Extracted sclera features with (a) high and (b) poor discrimination with iris region.

(ZMs) at different radii to classify each pixel into iris or noniris category. ZMs have been shown to constitute discriminant features for the image representation since they are less sensitive to noise and the information redundancy. The complete orthogonal and rotation invariance properties of the ZMs are effectively exploited in the proposed segmentation approach for the noisy iris images acquired under visible illumination in unconstrained environments. The scale invariance in the feature representation is inherently addressed during the mapping process from a localized iris region to a unit circle. One of the important features of the proposed iris segmentation approach is its ability to segment iris images acquired under varying illumination bands and, therefore, offers a

unified solution for the iris segmentation.

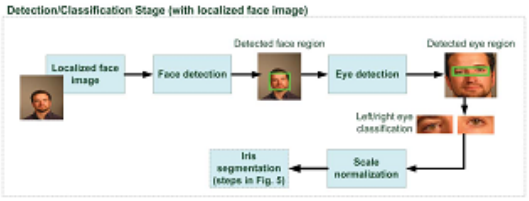

Fig. 4. Block diagram of proposed iris segmentation method with localized face image.

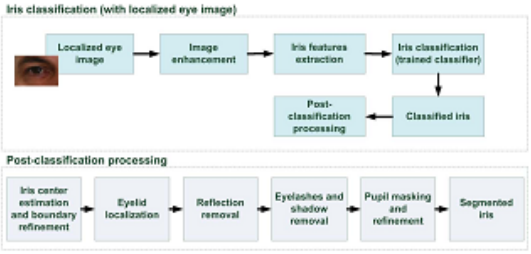

Fig. 5. Block diagram of proposed iris segmentation method with localized eye image.

The post classification processing is shown to be highly effective in reducing the segmentation error. Rigorous experiments were performed on two kinds of publicly available databases: 1) databases with localized face images (FRGC and CASIA.v4 iris-at-a-distance (hereafter referred to as CASIA.v4-distance)) and 2) database with localized eye regions (UBIRIS.v2 iris database). In the first case, face region is automatically localized by using AdaBoost-based face detector followed by an AdaBoost-based eye pair detector to localize the eyes. The performance comparison between the NN and support-vector-machine (SVM)-based classifiers using the segmentation method is reported from the extensive experiments to ascertain the adaptability of the developed approach to different imaging environment/databases.

3. IRIS SEGMENTATION FOR IMAGES ACQUIRED IN VISIBLE AND NIR ILLUMINATION

The iris segmentation approach developed in this paper is motivated by the work. The segmentation approach adopts pixel-based strategy to classify each pixel into iris/noniris category. Figs. 4 and 5 show the block diagrams of the proposed iris segmentation approach for both localized eye and face images. The proposed segmentation approach can be divided into two stages: 1) training/classification and 2) post classification. In this paper, a set of postclassification processing operations are developed (Section III-B) to further complement the trained classifier, in order to further refine the classified output. The postclassification processing operations are shown to be highly effective to further reducing the average segmentation error.

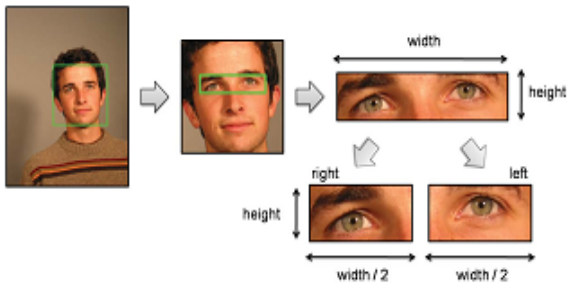

Fig. 6. Hierarchical face-eye detection.

3.1. Detection/Classification

3.1.1. Face and Eye Detection: Automated segmentation of eye region images, from the given face images in our experiments, is illustrated in Fig. 6. A hierarchical detection strategy is adopted by firstly detecting the face region. An eye-pair detector is then applied on the localized face region. The hierarchical detection approach improves the robustness to detect the eye region by confining the region of interest at each level, as compared to applying a single eye-pair detector.In this paper, AdaBoost-based face and eye-pair classifiers are employed for face and eye detection. The resulting output from the AdaBoost-based eye-pair detector is further refined by classifying each eye into left or right eye category. The left or right eye classification is simply partitioning the width of the detected eye-pair region: the first half as right eye and the second half as left eye.

3.1.2. Image Enhancement: Illumination variation poses the difficulties for both iris segmentation and recognition. The influence of the illumination conditions is even more noticeable when the acquisition is performed in the unconstrained environments using visible imaging. Although the problem has usually been addressed, none of the approaches provides the solution especially in the context of iris segmentation for images acquired in the unconstrained environments using visible imaging. For that reason, we propose to take the advantages of single scale retinex (SSR) algorithm for improving colour consistency regardless of illumination variation. The mathematical form for the SSR is as follows:

$$R_{i\in\{R,G,B\}}(x_1, x_2) = \log \frac{I_i(x_1, x_2)}{G_\sigma * I_i(x_1, x_2)} \qquad (1)$$

This mathematical form of SSR gives the result of colour consistency in the unconstrained environments.

IJSER

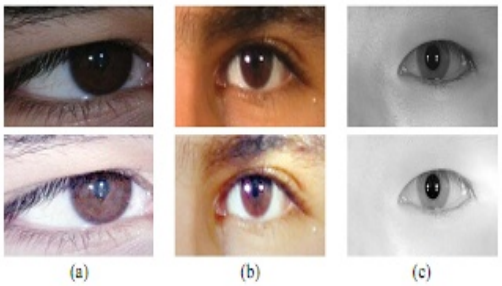

Fig. 7. Image enhancement using SSR image samples from (a) UBIRIS.v2, (b) FRGC, and (c) CASIA.v4-distance.

3.1.3. Feature Extraction: Localized texture description based on ZMs has been shown to outperform other alternatives in terms of noise resilience, information redundancy, and image representation. Therefore, ZM is used as the feature extractor to compute higher order local pixel dependencies in the local region. We extracted six features for every pixel at location (x1, x2) from a given image I in the local region represented by multiple radii. The most important approach of this feature extraction is to classifying the images.

The computed feature vector is of 6-D and is defined as follows:

$$\{x_1, x_2, I(x_1, x_2), Z^l_{mn}(I, x_1, x_2)\} \quad (2)$$

Where I represents single channel of enhanced eye image. Therefore, conversion of the colour image to the single-channel image is required, for example, the images acquired using visible imaging. In order to meet such requirement, the red channel of the colour image is employed this particular channel is utilized due to its spectral proximity toward NIR wavelength, which is commonly employed to acquire discriminative iris feature. Z is a function of I cantered at (x1, x2), which used to calculate the ZM at radius l ∈{2, 5, 7}.The ZMof order m ∈ N (m) and repetition n ∈ Z can be calculated using

$$Z^l_{mn} = \frac{m+1}{\pi} \sum_{x=x_1-l}^{x=x_1+l} \sum_{y=x_2-l}^{y=x_2+l} f(x,y)[V_{mn}(r,\theta)]^*. \quad (3)$$

The Zernike order to satisfy the missetto 4and6for VWandNIR databases, respectively, and the repetition n is set to zero for databases from both wavelengths.6 The function f denotes the extracted local region/sub image which is mapped to a unit circle, i.e., (x2 + y2 ≤ 1). The Zernike polynomials V across the radius r ∈[0, 1]: r ∈ R in the polar form is where n is subject to the conditions such that, m −|n| is even and |n|≤ m. The radial term in (4) is given as

$$V_{mn} = R_{mn}(r)e^{in\theta} \quad (4)$$

The constructed histogram is divided into ten equally spaced bins as we assume the intensity values in the localized iris region are highly similar since most of the artifacts such as reflection, ES have been eliminated with the prior postprocessing operations.

where n is subject to the conditions such that, m −|n| is even and |n|≤ m. The radial term in (4) particular channel is due to given as

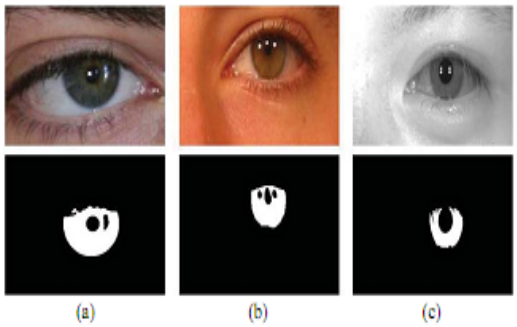

Fig. 8. Sample training images and corresponding manually labeled masks from database. (a) UBIRIS.v2, (b) FRGC, and (c) CASIA.v4-distance.

$$R_{mn}(r) = \sum_{s=0}^{\frac{(m-|n|)}{2}} (-1)^s \frac{(m-s)!}{s!\left(\frac{m+|n|}{2}-s\right)!\left(\frac{m-|n|}{2}-s\right)!} r^{m-2s}. \quad (5)$$

3.1.4. Training and Classification: The goal of classification is to find a generalized solution which can optimally separate the data into their corresponding classes/categories. SVM offers a computationally simpler model to obtain the solution which is global minimum and unique, as compared to NN.However, the performance comparison of each algorithm to solve the classification problem for iris segmentation has not yet been reported. In this paper, two commonly used supervised machine learning approaches—feed forward neural network (FNN) and SVM—are evaluated in order to show the adaptability to each different database used in our experiments. Both the classifiers are trained with the same training images, which are independent from the test images. Therefore, conversion of the colour image to the single-channel image is required, for example, the images acquired using visible imaging. The differences are due to the fact that the generalization performance of an SVM is less dependent on the training data and is fully determined by the support vectors.

The information used in learning for both FNN and SVM are summarized in Tables II and III, respectively.

IJSER

TABLE II

TRAINING CONFIGURATIONS FOR FNN-BASED CLASSIFIERS

	UBIRIS.v2	FRGC	CASIA.v4-distance
Total number of train images	41	40	41
No. of features per pixel	6		
No. of +/− samples	25 000/25 000		
No. of layers and neurons	6-11-1	6-11-1	6-9-1
Radii for windows (pixels)	2, 5, 7		
Order of Zernike moments	4		6
Learning algorithm	Levenberg-Marquardt		

TABLE III

TRAINING CONFIGURATIONS FOR SVM-BASED CLASSIFIERS

	UBIRIS.v2	FRGC	CASIA.v4-distance
Total number of train images	41	40	41
No. of features per pixel	6		
No. of +/− samples	10 000/10 000	10 000/10 000	10 000/10 000
Radii for windows (pixels)	2, 5, 7		
Order of ZMs	4		6
Kernel function	RBF		

Table III suggests that the least amount of positive and negative training samples7 are used for training the SVM classifiers as compared to FNN. The differences are due to the fact that the generalization performance of an SVM is less dependent on the training data and is fully determined by the support vectors. Classification of iris pixels is performed by using the trained classifier, as described above. Features are extracted for each pixel in a similar manner as in learning phase to form a collection of feature vectors. The set of feature vectors is fed into the trained classifier to induce labels (iris/noniris) for each pixel.

3.2. Postclassification Processing

The operations developed in this section play a vital role to further refine the classification results produced by the trained NN/SVM classifier. The pixels classified by the trained NN/SVM classifier often include noise resulting from false-negative and false-positive errors in the classification stage. Therefore, the robust postclassification processing steps are developed to mitigate the errors and improve the segmentation accuracy of the algorithm.

3.2.1. Iris Centre Estimation and Boundary Refinement: Iris centre is estimated by fitting a circle to an edge map generated

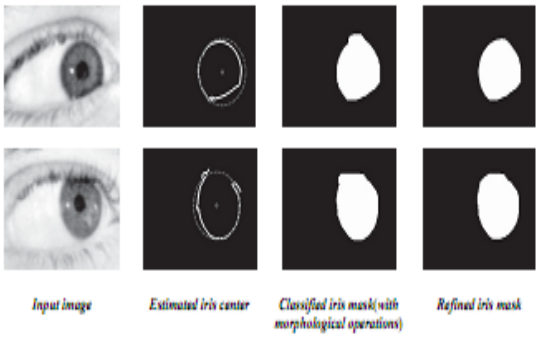

Fig. 9. Examples of iris center estimation and boundary refinement.

Using the classified iris mask which is firstly processed with morphological operations. The holes (pupil/reflection in the classified iris masks) are filled to obtain better estimation of iris centre by minimizing the influence from the pupil and reflection regions. There are two parameters required for the operation: 1) initial iris centre and 2) range of radius, which both can be easily estimated from the classified binary iris mask B. The initial centre (Cx1, Cx2) is estimated by calculating the centre of mass of B. For estimating the range of radius r , one can utilize the width and height information of B. In this paper, we consider only the height information h, which is least sensitive to the presence of eyelashes spread horizontally. The radius r can be computed as follows:

$$\{r \in N : \alpha h \le r \le \beta h, \alpha, \beta \in R, \alpha \le \beta, \alpha, \beta > 0\}. \quad (6)$$

After obtaining the necessary parameters, the best-fitted circle is searched within a small offset (±15 pixels) from the (Cx1, Cx2). The pixels in B which are fallen outside the best-fitted circle are removed, resulting in a boundary-refined iris mask, as shown in Fig. 9.

3.2.2. Eyelid Localization: The estimated iris centre (Cx1,Cx2) and the radius r obtained in the previous step are employed here. The iris centre serves as a reference point to partition the localized iris into two regions: upper and lower eyelid regions, which are delimited by r. Both upper and lower eyelids can be localized in a similar manner. Thus we explicate the localization approach by using the upper eyelid as an example. The key idea of the eyelid localization is to fit a polynomial curve with degree 2 to the candidate eyelid points extracted from an edge map generated using Canny edge detector. Considering the fact that

the intensity of eyelashes is usually darker than the skin and iris regions, robustness to extract the candidate eyelid points can be improved by exploiting the intensity information of an input image I simultaneously. The average column wise intensity information, μ1 and μ2, delimited by P pixels from an edge point (Ex1 , Ex2)

$$\mu_1 = \frac{1}{p}\sum_{x_2'=x_2-p}^{x_2-1} I(E_{x_1}, E_{x_2'}); \quad \mu_2 = \frac{1}{p}\sum_{x_2'=x_2+1}^{x_2+p} I(E_{x_1}, E_{x_2'})$$

are computed. (Ex1, Ex2) is considered a rightful candidate if μ1, μ2 > 1I (Ex1, Ex2) is satisfied. Furthermore, we adopted the strategy in to consider only one edge point per column wise, which can further mitigate the effect from the outlier. Fig. 10 presents some samples of the eyelid localization results.

4. CONCLUSION

1. A unified framework for completely automated iris segmentation using images acquired in both visible and NIR imaging was presented. The proposed approach exploited the higher order pixel relationship in a local region using ZMs and performed the pixel-based classification using trained NN/SVM classifier. In particular, the pixel-based classification addresses the problem of conventional segmentation approaches for segmenting images acquired at a distance and under unconstrained environments. Experimental results (Tables V and VI) presented on three publicly available databases in Section IV-B1 illustrated better performance than the previously proposed approaches for the VW imaging iris segmentation. The presented results suggested significant improvement in the average segmentation error by 47.5%, 34.1%, and 32.6% over the previously proposed approaches.

2. The developed framework incorporated robust post classification processing operations detailed in Section III-B.These developed operations were found to be highly efficient to mitigate the classification errors from the classification stage. These important steps were found not to be comprehensive in the previous approaches. When applying the developed postclassification processing to the classification results obtained using, the segmentation errors could be further improved by 34.7%, 10.3%, and 25.5% for UBIRIS.v2, FRGC, and CASIA.v4-distance databases, respectively. The presented results not only confirmed the effectiveness of the developed techniques but also suggested potential adaptability of the developed techniques to other segmentation approaches to further refine the segmentation results. In this paper, we consider only the height information and the process of segmentation.

3. Image enhancement using SSR was employed in this paper to account for the illumination variation problem. SSR is a colour constancy algorithm which helps alleviate the influence of the varying illumination to the iris segmentation problem. Illumination variation is often significant in the images acquired under unconstrained environments. Although such problem was discussed in the previous approaches, no efforts were made to address this problem.

REFERENCES

[1] K. Bowyer, K. Hollingsworth, and P. Flynn, "Image understanding for iris biometrics: A survey," *Image Vis. Comput.*, vol. 110, no. 2, pp. 281– 307, May 2008.
[2] J. Daugman, "How iris recognition works," *IEEE Trans. Circuits Syst. Video Technol.*, vol. 14, no. 1, pp. 21–30, Jan. 2004.
[3] H. Proenca, "Iris recognition: On the segmentation of degraded images acquired in the visible wavelength," *IEEE Trans. Pattern Anal. Mach. Intell.*, vol. 32, no. 8, pp. 1502–1516, Aug. 2010.
[4] N. Kourkoumelis and M. Tzaphlidou, "Medical safety issues concerning the use of incoherent infrared light in biometrics," in *Ethics and Policy Biometrics* (Lecture Notes in Computer Science), vol. 6005. Berlin, Germany: Springer-Verlag, Jan. 2010, pp. 121–126.
[5] H. Proenca, S. Filipe, R. Santos, J. Oliveira, and L. Alexandre, "The UBIRIS.v2: A database of visible wavelength images captured on the move and at-a-distance," *IEEE Trans. Pattern Anal. Mach. Intell.*, vol. 32, no. 8, pp. 1529–1535, Aug. 2010.
[6] H. Proenca and L. Alexandre, "UBIRIS: A noisy iris image database," in *Proc. Int. Conf. Image Anal. Process.*, vol. 1. Sep. 2005, pp. 970–977.
[7] S. Venugopalan, U. Prasad, K. Harun, K. Neblett, D. Toomey, J. Heyman, and M. Savvides, "Long range iris acquisition system for stationary and mobile subjects," in *Proc. Int. Joint Conf. Biometrics*, Washington, DC, Oct. 2011, pp. 1–20.
[8] J. Daugman, "New methods in iris recognition," *IEEE Trans. Syst. Man Cybern. B, Cybern.*, vol. 37, no. 5, pp. 1167–1175, Oct. 2007.
[9] S. A. Schuckers, N. Schmid, A. Abhyankar, V. Dorairaj, C. Boyce, and L. Hornak, "On techniques for angle compensation in nonideal iris recognition," *IEEE Trans. Syst. Man Cybern. B, Cybern.*, vol.37.
[10] *Information Technology–Biometric Data Interchange Formats–Part 6: Iris Image Data*, ISO/IEC Standard 19794–6, 2005.